ELSEVIER

0141-1187(94)00029-8

Applied Ocean Research **16** (1994) 363–372

0141-1187/94/$07.00

Finite element analysis of two-dimensional non-linear transient water waves

G. X. Wu

Department of Mechanical Engineering, University College London, Torrington Place, London, UK, WC1E 7JE

&

R. Eatock Taylor

Department of Engineering Science, University of Oxford, Parks Road, Oxford, UK, OX1 3PJ

(Received 12 January 1994; revised version received and accepted 3 November 1994)

The two-dimensional nonlinear time domain free surface flow problem is analyzed by the finite element method. Two approaches are used. One is based on the velocity potential which is approximated by means of shape functions. The solution is obtained through use of a variational statement, and the velocity is obtained subsequently by the Galerkin method. The other approach is to write both potential and velocity in terms of the shape functions at the same time. Their solutions are derived from the same equation by using another variational statement. Numerical results are given for the vertical wave maker problem and for a transient wave in a rectangular container. They are compared with analytical solutions, and very good agreement is found.

1 INTRODUCTION

In many cases the motion characteristics of a marine structure can be predicted by linearized velocity potential theory. In other cases, second order theory may be required. The TLP is a well known example of the latter. One of its typical design characteristics is that its resonant frequency is kept away from the region in which the dominating wave energy exists. This avoids excessive motions being caused by the linear wave forces. Such design practice, however, leads to the motions due to second order forces being of particular importance. For motions in the horizontal plane (surge, sway and yaw), the resonant frequency is low. The second order slowly varying (difference-frequency) wave forces may cause a large drift of the structure from its mean position. For the motions in the vertical plane (heave, roll and pitch), the resonant frequency is high, and second order sum-frequency wave forces may cause significant response (springing).

There are also many applications of potential flow theory in the offshore industry which are well beyond the scope of the linear and second order analysis. A typical example is the so-called 'ringing' phenomenon. It is believed that this can cause high stresses or other undesirable effects, and preliminary investigations have indicated that steep transient waves may be the cause. The calculation of the loading on the structure by this type of wave involves the solution of the fully nonlinear free surface wave problem in the time domain.

The two-dimensional time domain nonlinear problem has received considerable attention in recent years.[1–7] The analysis has been mainly based on the boundary element method. Although significant progress has been made, success of this technique for the full three-dimensional analysis of a practical structure is limited. Several difficulties exist in this method. The combined effect of the singularity on the waterline and the singularity in the boundary integral equation requires particular attention. Another difficulty is that the boundary element method is limited to the case of potential flow. It may be modified to represent viscous flows, but the fluid domain must also be discretized in this case,[8] and many of the advantages of the method are then lost. The finite difference method may provide an alternative,[9,10] but here we use the finite element method. This is likely to have significant advantages in the case of complex geometries, where it is desirable to be able to use unstructured meshes.

In this paper we consider the two-dimensional problem, based on the potential flow theory. The

differential equations are satisfied through a variational statement. Two different methods are used. The first uses a conventional finite element technique, whereas the second uses a mixed element method. In the latter, both the velocity potential and velocity itself are expressed in terms of the shape functions, and both appear in the variational statement. The advantages and disadvantages of these two formulations are compared. This enables us to choose an efficient and accurate method for application to the three-dimensional problem.

2 MATHEMATICAL FORMULATION

We define a Cartesian coordinate system $O-xy$ such that the origin is on the mean free surface and y points vertically upwards. The fluid is assumed to be incompressible and inviscid, and flow is assumed to be irrotational. A velocity potential ϕ can then be introduced, which satisfies the Laplace equation

$$\nabla^2\phi = 0 \tag{1}$$

in the fluid domain R. The domain is partly bounded by a rigid surface S_2 (the body), on which the boundary condition is

$$\frac{\partial\phi}{\partial n} = f_2 \tag{2}$$

Here f_2 is the normal velocity of the body surface and $\boldsymbol{n}$ is the normal of the surface pointing out of the fluid domain. The boundary conditions on the free surface S_1 or $y = \eta$ can be written as

$$g\eta + \frac{\partial\phi}{\partial t} + \frac{1}{2}\nabla\phi\cdot\nabla\phi = 0 \tag{3a}$$

$$\frac{\partial\phi}{\partial y} = \frac{\partial\eta}{\partial t} + \frac{\partial\phi}{\partial x}\frac{\partial\eta}{\partial x} \tag{3b}$$

where g is the gravitational acceleration and t is time. Equations (3) may also be written in the Lagrangian form

$$\frac{\mathrm{d}\phi}{\mathrm{d}t} = g\eta - \frac{1}{2}\nabla\phi\nabla\phi \tag{4}$$

$$\frac{\mathrm{d}x}{\mathrm{d}t} = \frac{\partial\phi}{\partial x}, \qquad \frac{\mathrm{d}y}{\mathrm{d}t} = \frac{\partial\phi}{\partial y} \tag{5}$$

The initial conditions at $t = 0^+$ are given as

$$\phi(x, y = \xi, t = 0) = \psi(x) \qquad \eta(x, t = 0) = \xi(x) \tag{6}$$

We use a finite difference procedure to advance the solution in the time domain. Thus we assume that the potential on the free surface at time t is f_1 (i.e. $f_1 = \psi(x)$, when $t = 0$). Once the solution at time t has been found, the potential on the new free surface profile at a subsequent time $t + \Delta t$ can be obtained using eqns (4) and (5). This provides the free surface condition at $t + \Delta t$, and the problem can be solved again. For example, one could use the following equations

$$x|_{t+\Delta t} = x|_t + \left(\frac{\mathrm{d}x}{\mathrm{d}t}\right)_t \Delta t$$

$$y|_{t+\Delta t} = y|_t + \left(\frac{\mathrm{d}y}{\mathrm{d}t}\right)_t \Delta t \tag{7a}$$

$$\phi|_{t+\Delta t} = \phi|_t + \left(\frac{\mathrm{d}\phi}{\mathrm{d}t}\right)_t \Delta t \tag{7b}$$

To improve accuracy and stability a more sophisticated procedure than this, such as the fourth order Runge–Kutta method, could also be used (as in the results given below).

3 FINITE ELEMENT METHOD (FEM)

The above formulation shows that the problem at each time step is of the mixed Neumann and Dirichlet type. To obtain a numerical solution, we first consider the following functional

$$\Pi_1 = \frac{1}{2}\int_R \nabla\phi\nabla\phi\,\mathrm{d}R - \int_{S_2}\phi f_2\,\mathrm{d}S - \int_{S_1}\frac{\partial\phi}{\partial n}(\phi - f_1)\,\mathrm{d}S \tag{8}$$

The variational statement

$$\delta\Pi_1 = 0 \tag{9}$$

leads to

$$\begin{aligned}
&\int_R \nabla\delta\phi\nabla\phi\,\mathrm{d}R - \int_{S_2}\delta\phi f_2\,\mathrm{d}S - \int_{S_1}\frac{\partial\delta\phi}{\partial n}(\phi - f_1)\,\mathrm{d}S \\
&\quad - \int_{S_1}\frac{\partial\phi}{\partial n}\delta\phi\,\mathrm{d}S \\
&= \int_R \nabla(\delta\phi\nabla\phi)\,\mathrm{d}R - \int_R \delta\phi\nabla^2\phi\,\mathrm{d}R \\
&\quad - \int_{S_2}\delta\phi f_2\,\mathrm{d}S - \int_{S_1}\frac{\partial\delta\phi}{\partial n}(\phi - f_1)\,\mathrm{d}S - \int_{S_1}\frac{\partial\phi}{\partial n}\delta\phi\,\mathrm{d}S \\
&= -\int_R \delta\phi\nabla^2\phi\,\mathrm{d}R + \int_{S_2}\delta\phi\left(\frac{\partial\phi}{\partial n} - f_2\right)\mathrm{d}S \\
&\quad - \int_{S_1}\frac{\partial\delta\phi}{\partial n}(\phi - f_1)\,\mathrm{d}S \\
&= 0
\end{aligned} \tag{10}$$

This is equivalent to the governing equation and boundary conditions on ϕ at each time step.

We now divide the fluid domain into finite elements. The velocity potential can be written as

$$\phi = \sum_{j=1}^{n}\phi_j N_j(x, y) \tag{11}$$

where ϕ_j are the nodal values of the potential, n is the number of the nodes and $N_j(x, y)$ are the shape

functions. Substituting this equation into (8) and using (9), we obtain

$$\int_R \nabla N_i \sum_{j=1}^{n} \phi_j \nabla N_j \, dR - \int_{S_2} N_i f_2 \, dS - \int_{S_1} \frac{\partial N_i}{\partial n} \left(\sum_{j=1}^{n} \phi_j N_j - f_1 \right) dS - \int_{S_1} N_i \sum_{j=1}^{n} \phi_j \frac{\partial N_j}{\partial n} dS = 0 \tag{12}$$

In matrix form, this can be written as

$$[A][\phi] = [B] \tag{13}$$

where the coefficients may be given as

$$A(i,j) = \int_R \nabla N_i \nabla N_j \, dR - \int_{S_1} \frac{\partial (N_i N_j)}{\partial n} dS \tag{14}$$

$$B(i) = \int_{S_2} N_i f_2 \, dS - \int_{S_1} \frac{\partial N_i}{\partial n} f_1 \, dS \tag{15}$$

Solution of eqn (13) then provides an approximation to the velocity potential. But eqns (4) and (5) also require the velocity. Although it is convenient to obtain the velocity by differentiating the shape functions with respect to the coordinates, the shape functions usually do not guarantee the continuity of its derivatives at the boundaries of the elements. On the other hand, accurate prediction of the velocity is important to avoid excessive accumulated error in the time-stepping procedure. Thus we use the following method.

The velocity vector $\boldsymbol{u} = u\boldsymbol{i} + v\boldsymbol{j}$ is written in terms of the shape functions

$$\boldsymbol{u} = \sum_{j=1}^{n} \boldsymbol{u}_j N_j(x,y) \tag{16}$$

To impose the relationship

$$\nabla \phi = \boldsymbol{u} \tag{17}$$

we use the Galerkin method to approximate it in the form

$$\int_R N_i (\nabla \phi - \boldsymbol{u}) \, dR = 0 \tag{18}$$

Substituting eqns (11) and (16) into (18), we obtain

$$[C][u] = [D_1][\phi] \qquad [C][v] = [D_2][\phi] \tag{19}$$

where the coefficients of the matrix are given as

$$C(i,j) = \int_R N_i N_j \, dR \qquad D_1(i,j) = \int_R N_i \frac{\partial N_j}{\partial x} dR \qquad D_2(i,j) = \int_R N_i \frac{\partial N_j}{\partial y} dR \tag{20}$$

and u_i and v_i are the components of the velocity vector of $\boldsymbol{u}_j$ at node j.

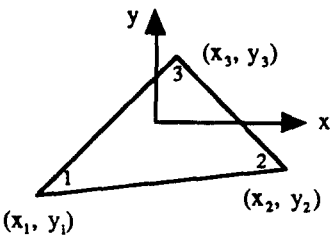

Fig. 1. Triangular finite element.

From the resulting values of velocity, we can obtain the updated position of the free surface at the start of the next time step using eqn (5); and the updated velocity potential on the free surface is obtained from eqn (4). A new finite element mesh may then be generated, corresponding to the updated geometry.

In what follows we use triangular elements as shown in Fig. 1. Linear shape functions are adopted, which are defined as

$$N_p(x,y) = (\alpha_p + \beta_p x + \gamma_p y)/2\Delta, \tag{21}$$

where Δ is the area of the element and

$$\alpha_1 = x_2 y_3 - x_3 y_2 \qquad \alpha_2 = x_3 y_1 - x_1 y_3 \qquad \alpha_3 = x_1 y_2 - x_2 y_1 \tag{22a}$$

$$\beta_1 = y_2 - y_3 \qquad \beta_2 = y_3 - y_1 \qquad \beta_3 = y_1 - y_2 \tag{22b}$$

$$\gamma_1 = x_3 - x_2 \qquad \gamma_2 = x_1 - x_3 \qquad \gamma_3 = x_2 - x_1 \tag{22c}$$

The contribution of this element to the global matrix $[A]$ in eqn (13) then becomes

$$a(p,q) = (\beta_p \beta_q + \gamma_p \gamma_q)/4\Delta + a'(p,q) \qquad (p,q = 1,2,3) \tag{23}$$

The last term in this equation exists only when the element is attached to the free surface S_1. Assume that the rth side of the element is part of S_1, and that p_1 and p_2 are the two nodes joined by this side while p_3 is the other node belonging to the element. These terms can then be given as

$$\begin{cases} a'(p_1,p_2) = a'(p_2,p_1) = -(\beta_{p_3}^2 + \gamma_{p_3}^2)/4\Delta \\ a'(p_{1(2)},p_{1(2)}) = (\beta_{p_{1(2)}}\beta_{p_3} + \gamma_{p_{1(2)}}\gamma_{p_3})/4\Delta \\ a'(p_1,p_3) = a'(p_2,p_3) = (\beta_{p_3}^2 + \gamma_{p_3}^2)/4\Delta \\ a'(p_3,p_3) = 0 \end{cases} \tag{24}$$

where $p_{i(j)}$ denotes p_i or p_j.

4 MIXED FINITE ELEMENT METHOD (MFEM)

As discussed above, the accurate calculation of the velocity is crucial if excessive accumulated error is to be avoided. This has led us to investigate whether a mixed method will provide more accurate results. Rather than using eqn (1), we can start directly from the conditions

of irrotational flow and continuity. Thus we use:

$$\nabla\phi = \boldsymbol{u} \tag{25a}$$

$$\nabla\cdot\boldsymbol{u} = 0 \tag{25b}$$

Correspondingly, the boundary conditions can be written as

$$\phi = f_1 \tag{26}$$

on S_1 at each time step, and

$$\boldsymbol{u}\cdot\boldsymbol{n} = f_2 \tag{27}$$

on S_2.

We then develop the numerical analysis retaining $\boldsymbol{u}$ and ϕ as independent variables. In place of eqn (8), we consider the following functional

$$\Pi_2 = \int_R \phi\nabla\cdot\boldsymbol{u}\,\mathrm{d}R + \frac{1}{2}\int_R \boldsymbol{u}\cdot\boldsymbol{u}\,\mathrm{d}R - \int_{S_2}\phi(\boldsymbol{u}\cdot\boldsymbol{n} - f_2)\,\mathrm{d}S - \int_{S_1} f_1\boldsymbol{u}\cdot\boldsymbol{n}\,\mathrm{d}S \tag{28}$$

The variational statement

$$\delta\Pi_2 = 0 \tag{29}$$

leads to

$$\begin{aligned}
&\int_R(\delta\phi\nabla\cdot\boldsymbol{u} + \phi\nabla\cdot\delta\boldsymbol{u})\,\mathrm{d}R + \int_R \boldsymbol{u}\cdot\delta\boldsymbol{u}\,\mathrm{d}R \\
&\quad - \int_{S_2}[\delta\phi(\boldsymbol{u}\cdot\boldsymbol{n} - f_2) + \phi\delta\boldsymbol{u}\cdot\boldsymbol{n}]\,\mathrm{d}S - \int_{S_1} f\delta\boldsymbol{u}\cdot\boldsymbol{n}\,\mathrm{d}S \\
&= \int_R \delta\phi\nabla\cdot\boldsymbol{u}\,\mathrm{d}R + \int_R \nabla\cdot(\phi\delta\boldsymbol{u})\,\mathrm{d}R \\
&\quad + \int_R(\boldsymbol{u} - \nabla\phi)\cdot\delta\boldsymbol{u}\,\mathrm{d}R \\
&\quad - \int_{S_2}[\delta\phi(\boldsymbol{u}\cdot\boldsymbol{n} - f_2) + \phi\delta\boldsymbol{u}\cdot\boldsymbol{n}]\,\mathrm{d}S - \int_{S_1} f_1\delta\boldsymbol{u}\cdot\boldsymbol{n}\,\mathrm{d}S \\
&= \int_R \delta\phi\nabla\cdot\boldsymbol{u}\,\mathrm{d}R + \int_R(\boldsymbol{u} - \nabla\phi)\cdot\delta\boldsymbol{u}\,\mathrm{d}R \\
&\quad - \int_{S_2}\delta\phi(\boldsymbol{u}\cdot\boldsymbol{n} - f_2)\,\mathrm{d}S + \int_{S_1}(\phi - f_1)\delta\boldsymbol{u}\cdot\boldsymbol{n}\,\mathrm{d}S \\
&= 0
\end{aligned} \tag{30}$$

It is then easy to see that this equation is equivalent to eqns (25)–(27).

The representation of the velocity potential in eqn (11) is again used here, while the velocity is written as

$$\boldsymbol{u} = \sum_{j=1}^{n}\boldsymbol{u}_j M_j(x,y) \tag{31}$$

where the choice of shape function $M_j(x,y)$ in this equation does not have to be the same as $N_j(x,y)$. Substituting these expansions into eqn (28) and using (29), we obtain

$$\int_R \frac{\partial M_i}{\partial x}\sum_{j=1}^{n}\phi_j N_j\,\mathrm{d}R + \int_R M_i\sum_{j=1}^{n}u_j M_j\,\mathrm{d}R - \int_{S_2} M_i n_x\sum_{j=1}^{n}\phi_j N_j\,\mathrm{d}S - \int_{S_1} f_1 M_i n_x\,\mathrm{d}S = 0 \tag{32a}$$

$$\int_R N_i\sum_{j=1}^{n}\frac{\partial M_j}{\partial n}(u_j + v_j)\,\mathrm{d}R - \int_{S_2} N_i\left[\sum_{j=1}^{n}(u_j M_j n_x + v_j M_j n_y) - f_2\right]\mathrm{d}S = 0 \tag{32b}$$

$$\int_R \frac{\partial M_i}{\partial y}\sum_{j=1}^{n}\phi_j N_j\,\mathrm{d}R + \int_R M_i\sum_{j=1}^{n}v_j M_j\,\mathrm{d}R - \int_{S_2} M_i n_y\sum_{j=1}^{n}\phi_j N_j\,\mathrm{d}S - \int_{S_1} f_1 M_i n_y\,\mathrm{d}S = 0 \tag{32c}$$

where n_x and n_y are the components of the normal $\boldsymbol{n}$. In matrix form, these can be written as

$$\begin{bmatrix} A_{uu} & A_{u\varphi} & 0 \\ A_{\varphi u} & 0 & A_{uv} \\ 0 & A_{\varphi v} & A_{vv} \end{bmatrix}\begin{bmatrix} u \\ \phi \\ v \end{bmatrix} = \begin{bmatrix} B_u \\ B_\varphi \\ B_v \end{bmatrix} \tag{33}$$

where the coefficients of the sub-matrices are

$$A_{uu}(i,j) = \int_R M_j M_i\,\mathrm{d}R \tag{34a}$$

$$A_{u\varphi}(i,j) = \int_R N_j\frac{\partial M_i}{\partial x}\mathrm{d}R - \int_{S_2} N_j M_i n_x\,\mathrm{d}S \tag{34b}$$

$$A_{\varphi v}(i,j) = \int_R N_i\frac{\partial M_j}{\partial y}\mathrm{d}R - \int_{S_2} N_i M_j n_y\,\mathrm{d}S \tag{34c}$$

$$A_{\varphi u} = A_{u\varphi}^T \qquad A_{v\varphi} = A_{\varphi v}^T \qquad A_{vv} = A_{uu} \tag{34d}$$

$$B_u(i) = \int_{S_1} f_1 M_i n_x\,\mathrm{d}S \qquad B_\varphi(i) = -\int_{S_2} f_2 N_i\,\mathrm{d}S \qquad B_v(i) = \int_{S_1} f_1 M_i n_y\,\mathrm{d}S \tag{34e}$$

When the triangular element in Fig. 1 and linear shape functions have been chosen, the contributions of this element to the global matrix in eqn (33) become

$$a_{uu}(p,q) = \epsilon_{pq}\Delta/12 \tag{35a}$$

$$\begin{aligned} a_{u\varphi}(p,q) &= \beta_p/6 + a'_{u\varphi}(p,q) \\ a_{\varphi v}(p,q) &= \gamma_q/6 + a'_{\varphi v}(p,q) \end{aligned} \tag{35b}$$

where $\epsilon_{pq} = 1$ if $p \neq q$ and $\epsilon_{pq} = 2$ if $p = q$. The last terms of eqns (35b) and (30) exist only when the element

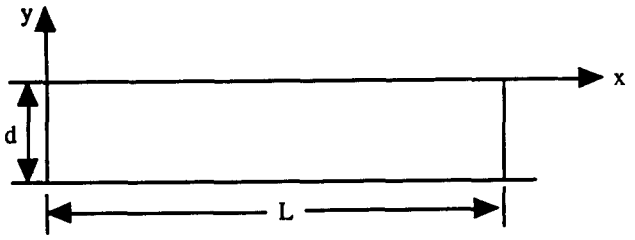

Fig. 2. Elevation of tank with wave maker at $x = 0$.

is attached to the free surface S_1. As with eqn (24), we obtain

$$\begin{cases} a'_{u\varphi}(p_1,p_2) = a'_{u\varphi}(p_2,p_1) = \beta_r/6 \\ a'_{u\varphi}(p_{1(2)},p_{1(2)}) = \beta_r/3 \\ a'_{u\varphi}(p_{1(2,3)},p_3) = a'_{u\varphi}(p_3,p_{1(2,3)}) = 0 \end{cases} \tag{36a}$$

$$\begin{cases} a'_{\varphi v}(p_1,p_2) = a'_{\varphi v}(p_2,p_1) = \gamma_r/6 \\ a'_{\varphi v}(p_{1(2)},p_{1(2)}) = \gamma_r/3 \\ a'_{\varphi v}(p_{1(2,3)},p_3) = a'_{\varphi v}(p_3,p_{1(2,3)}) = 0 \end{cases} \tag{36b}$$

5 RESULTS AND DISCUSSION

We first consider the problem of a wave maker in a tank with length L and depth d, as shown in Fig. 2. The various parameters are nondimensionalized by redefining them as follows

$$\phi \to d(gd)^{1/2}\phi \qquad (x,y) \to d(x,y) \qquad t \to (d/g)^{1/2}t \tag{37}$$

The wave maker is assumed to be suddenly set into motion with a constant speed U. It is then easy to confirm that in its dimensionless form $f_2 = U/\sqrt{(gd)} = \mathrm{Fn}$ on the wave maker, and $f_2 = 0$ on the bottom and the other side of the tank. Initially $f_1 = 0$ on the free surface and it is calculated from eqns (4) and (5) at subsequent time steps. The singularity[11,12] in this problem at $x = y = 0$ when $t = 0$ requires attention, this being due to the contradiction of the free surface boundary condition and the body surface boundary condition at the point of intersection.

Results at $t = 0^+$ were first obtained by solving eqn (13) directly. This was found to give quite good results for both the potential and velocity on the wave maker, but totally unrealistic results for the potential and wave elevation on the free surface. We believe that this is due to the above mentioned singularity, since we have discovered that the method gives very good results on the free surface for the problem in which the wave maker is stationary but the bottom moves upwards. It is known that when both the body surface condition and the free surface boundary conditions are imposed, the singularity at $x = y = 0$ will be removed from the numerical solution. Although these conditions are imposed in eqn (10), they are satisfied not at specified points but in an averaged sense via an integration over the relevant boundaries. This may not be able to remove the effect of the singularity entirely from the numerical solution. We have therefore made the following modification. As the potential on the free surface is specified at the start of each time step, we may replace those ϕ_j with f_1 at the corresponding points. As a result eqn (12) becomes

$$\int_R \nabla N_i \sum_{j=1}^{n} \phi_j \nabla N_j \, \mathrm{d}R\big|_{j \notin S_1} = \int_{S_2} N_i f_2 \, \mathrm{d}S - \int_R \nabla N_i \sum_{j=1}^{n} \phi_j \nabla N_j \, \mathrm{d}R\big|_{j \in S_1} \qquad i \notin S_1 \tag{38}$$

and $A(i,j)$ and $B(i)$ are modified accordingly for points i on the free surface.

Figures 3 and 4 give the results obtained from solution of the corresponding modified matrix equation when $\mathrm{Fn} = 1$ and $L = 10d$. They show the velocity potential and the vertical fluid particle velocity on the wave maker (Fig. 3a and b respectively), and the vertical velocity of the free surface, calculated using two different meshes. These employed 8 segments vertically and 25 horizontally, and twice as many in each direction. The results are compared with the analytical solution obtained by Peregrine[11] for $L = \infty$ and excellent agreement may be observed. Figures 3 and 4 also give results obtained from the MFEM by solving eqn (33) with the same meshes. This does not seem to give better results than the FEM.

Equation (33) could also be modified by moving those parameters given in the boundary conditions to the right hand side. But this has not been attempted, since the FEM incorporating eqn (38) already gives very good results while the MFEM requires much more memory and CPU. The results given below have all been obtained using the FEM with eqn (38).

Figure 5 gives results for the free surface elevation at subsequent times, based on $\Delta t = 0{\cdot}01$. The fourth order Runge–Kutta method was used for integration with respect to time. The numerical results are compared with the analytical approximation[11] which retains only the terms of order t. It can be seen that the agreement is excellent. Some difference appears when $t = 0{\cdot}2$, which may be due to the neglect of higher order terms in t in the analytical solution.

We now consider the time domain problem in a rectangular container with depth d and width b, for an initial free surface disturbance. The parameters have again been nondimensionalized as in eqn (37). The coordinate system is the same as that used in the case of the wave maker (Fig. 2). The problem can be solved analytically using the perturbation expansion method. In the Appendix, we derive the solution up to second

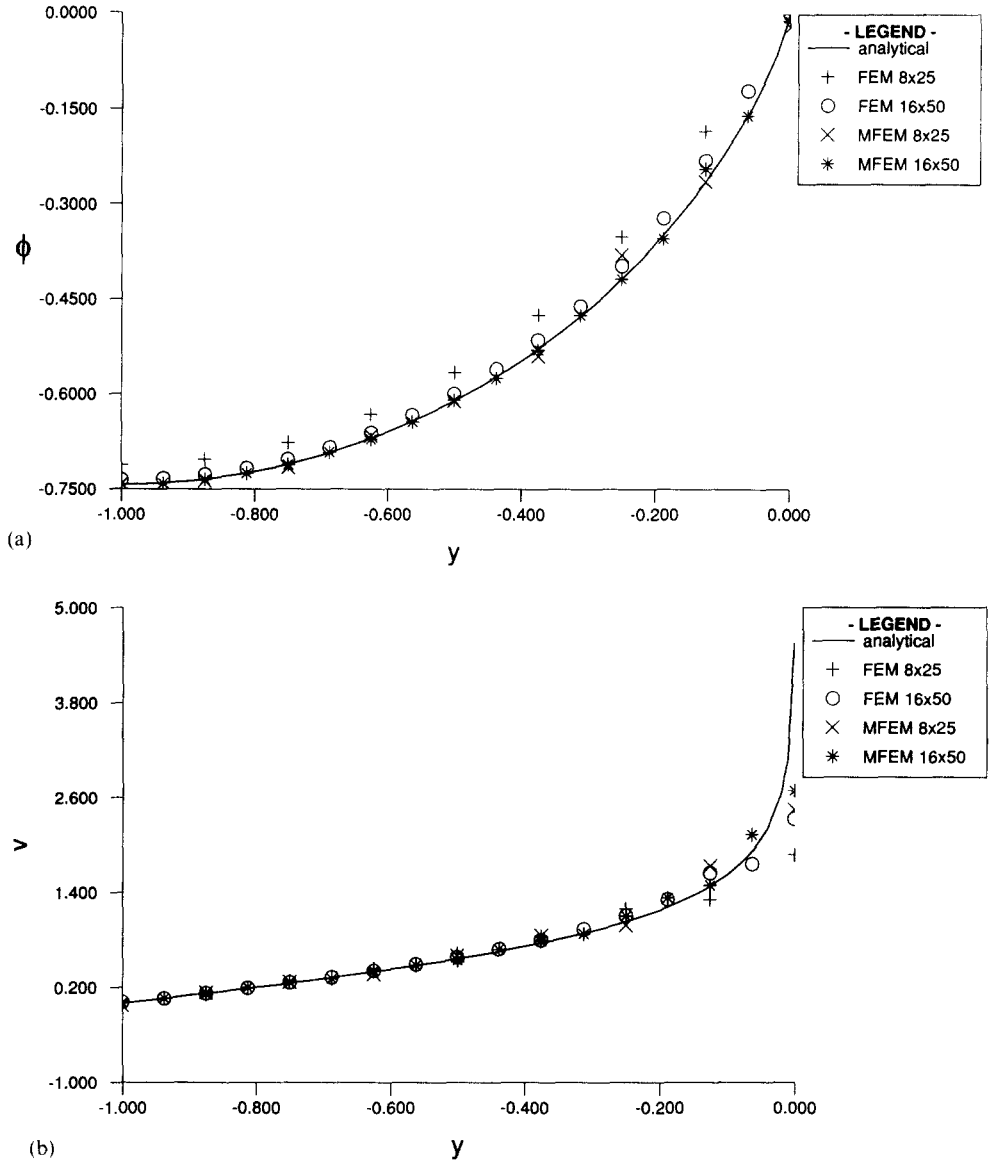

Fig. 3. Results at the wave maker ($x = 0$): (a) velocity potential; (b) vertical velocity.

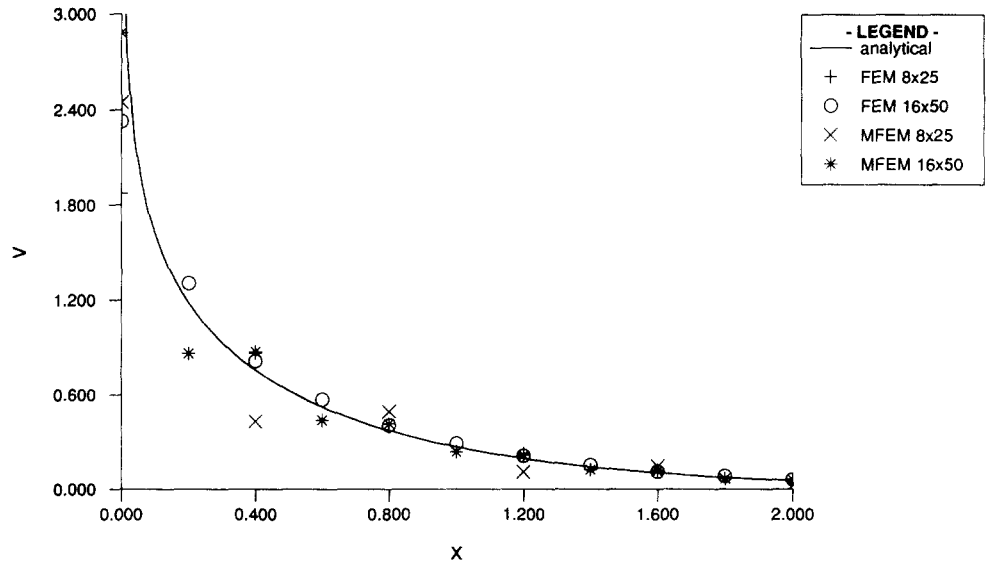

Fig. 4. Vertical velocity on the free surface immediately after starting the wave maker.

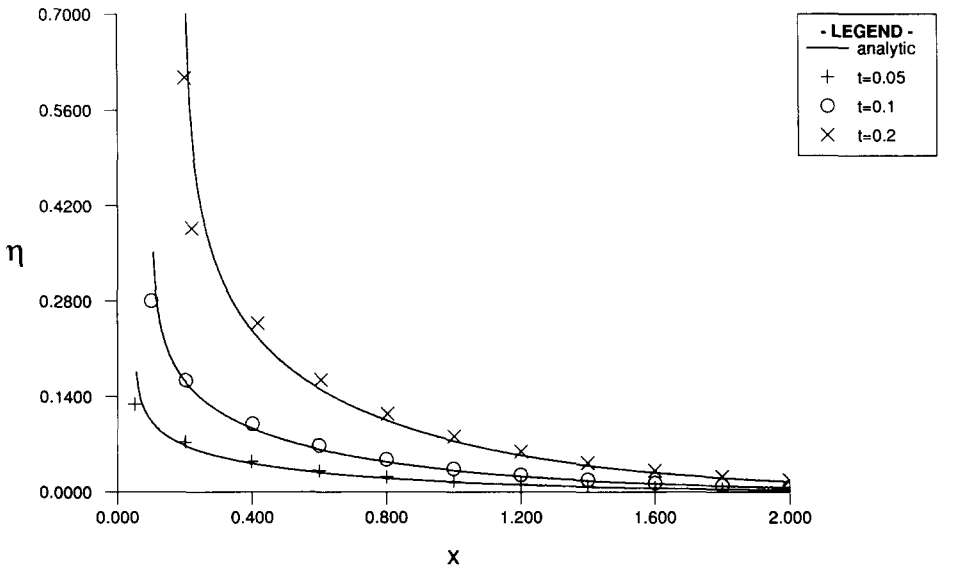

Fig. 5. Free surface elevation at successive time steps after starting the wave maker.

order, corresponding to the following initial wave elevation

$$\eta(x, t = 0) = a\cos(2\pi x/b) \tag{39}$$

Figures 6(a) and (b) give comparisons of the wave elevation η/a at the middle of the container ($x = b/2$), obtained from the numerical method and the analytical solution for two different amplitudes a. For these results $b = 2d$.

A typical initial mesh used in the numerical method is shown in Fig. 7. The container is divided uniformly in the x direction by $N + 1$ vertical lines at $x = x_j$, given by

$$x_j = (j - 1)b/N \qquad j = 1, 2, \ldots N + 1 \tag{40a}$$

On each of these lines, the $M + 1$ nodes are distributed exponentially in the y direction since the potential decays in this way, i.e.

$$y_{i,j} = d\frac{1 - \exp[\alpha(d + \eta_j)(M + 1 - i)/M]}{1 - \exp[\alpha(d + \eta_j)]} + \eta_j$$
$$i = 1, 2, \ldots M + 1 \tag{40b}$$

where η_j are obtained from eqn (30) with x being replaced by x_j. The choice of α in the equation depends on how fine the mesh is required to be near the free surface. At each time step, the mesh is regenerated by using eqn (40b), but now η_j is the wave elevation at x_j for the particular instant (x_j remains unchanged). The numerical results in Figs 6(a) and (b) are based on $\alpha = 2$ and two different mesh densities: $N = 32$, $M = 16$ (this corresponds to 561 nodes and 1024 triangular elements), and $N = 64$, $M = 32$ (2145 nodes and 5096 elements). The nondimensional time step is 0·2, and the smoothing technique used by Longuet-Higgins and Cokelet[13] has been applied in the calculation.

It is interesting to see from Fig. 6(a) that even when $a/d = 0{\cdot}05$, the linearized analytical solution still does not agree well with the fully nonlinear numerical solution as time increases. The inclusion of the second order solution, however, leads to a much improved agreement. Figure 6(b) gives a similar comparison for $a/d = 0{\cdot}1$. It shows that the agreement with the second order solution is not as good as that when $a/d = 0{\cdot}05$. This may be partly because the problem is more strongly nonlinear in this case. But there is another important point. Since a smoothing technique is used in the numerical solution, it effectively acts like viscous damping. As time increases, the energy in the container gradually reduces. Thus the numerical solution will eventually depart from the analytical solution based entirely on the potential theory (even if the latter were exact). We observe from the numerical calculations that the wave elevation does in fact decay as time increases. Furthermore, for the coarser mesh, the wave decays faster.

5 CONCLUSIONS

The two-dimensional nonlinear time domain free surface flow problem has been solved by the finite element method. The treatment of the singularity is crucial, and a successful method of dealing with this has been demonstrated. The scheme used in eqn (19) for calculating the velocity from the velocity potential has enabled linear shape functions to be used without sacrificing accuracy. The use of linear functions over triangular elements means that all integrations can be performed explicitly. This not only saves considerable computer time but also removes a possible source of error. The success of these schemes suggests that this approach can be extended to two- and three-dimensional analyses of non linear hydrodynamic problems associated with offshore structures.

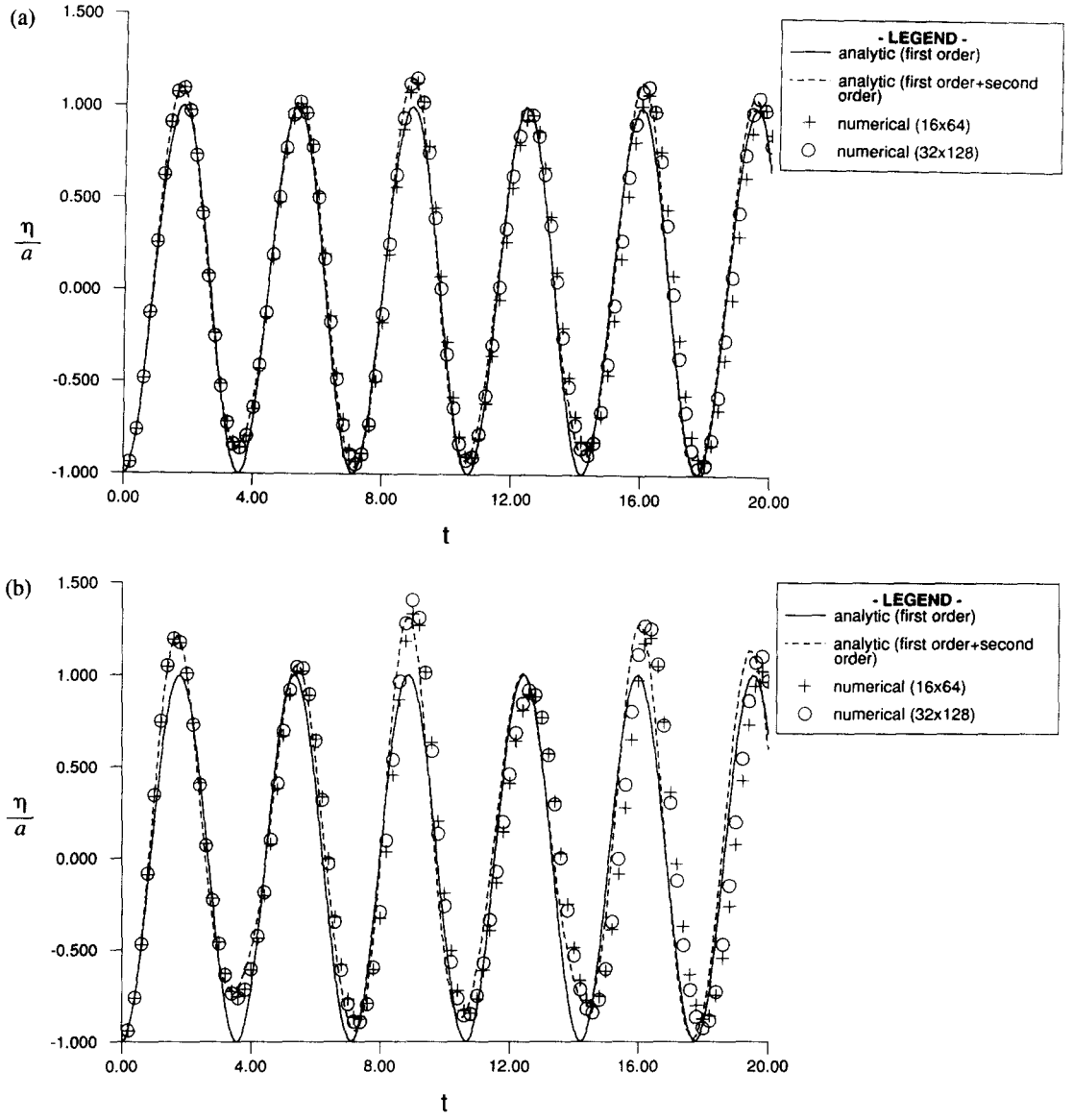

Fig. 6. Time history of elevation in a container: (a) $a/d = 0{\cdot}05$; (b) $a/d = 0{\cdot}10$.

Smoothing has been found necessary when the calculation extends over a long period of time. It acts, however, in a similar way to viscous damping: it gradually dissipates the energy within the fluid. A question, therefore, remains: does the introduction of the smoothing lead to a better solution compared with the physical reality, or is it merely an artificial scheme for obtaining a stable numerical solution. This clearly requires further investigation.

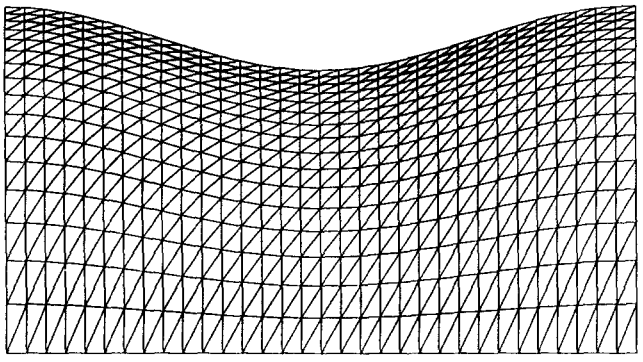

Fig. 7. Mesh at start for initial value problem in a container.

ACKNOWLEDGEMENT

This work forms part of the research programme "Uncertainties in Loads on Offshore Structures" sponsored by EPSRC through MTD Ltd and jointly funded with: Amoco (UK) Exploration Company, BP Exploration Operating Co Ltd, Brown & Root, Exxon Production Research Company, Health and Safety Executive, Norwegian Contractors a.s., Shell UK Exploration and Production, Den Norske Stats Oljeselskap a.s., Texaco Britain Ltd.

REFERENCES

1. Cointe, R., Geyer, P., King, B., Molin, B. & Tramoni, M., Nonlinear and linear motions of a rectangular barge in a perfect fluid. *Proc. 18th Symp. on Naval Hydrodynamics*, Michigan, USA, 1990, 85–98.
2. Grosenbaugh, M. A. & Yeung, R. W., Nonlinear bow flows — an experimental and theoretical investigation. *Proc. 17th Symp. on Naval Hydrodynamics*, The Hague, The Netherlands, 1988, 195–213.
3. Lin, W. M., Newman, J. N. & Yue, D. K., Nonlinear forced motion of floating bodies. *Proc. 15th Symp. on Naval Hydrodynamics*, Hamburg, Germany, 1984, 33–47.
4. Mori, K., New treating of the free-surface and downstream boundary conditions in numerical computations of free-surface flows. *Proc. 7th Int. Workshop on Water Waves and Floating Bodies*, Val de Reuil, France.
5. Tulin, M. P. & Yao, Y., Wavemaking by a large oscillating body near tank resonance. *Proc. 7th Int. Workshop on Water Waves and Floating Bodies*, Val del Reuil, France.
6. Van Daalen, E. F. G. & Huijsmans, R. H. M., On the impulsive motion of a wavemaker. *Proc. 6th Int. Workshop on Water Waves and Floating Bodies*, Woods Hole, USA, 1991.
7. Zhao, R. & Faltinsen, O. M., Water entry of two dimensional bodies. *J. Fluid Mech.*, **246** (1992) 593–612.
8. Price, W. G. & Tan, M.-Y., Fundamental viscous solutions or "transient oseenlets" associated with a body manoeuvring in a viscous fluid. *Proc. Roy. Soc. London*, A**438** (1992) 447–466.
9. Telste, J. G., Calculation of fluid motion resulting from large-amplitude forced heave motion of a two-dimensional cylinder in a free surface. *Proc. 4th Int. Conf. on Numerical Ship Hydrodynamics*, Washington, USA 1985, 81–93.
10. Yeung, R. W. & Vaidhanathan, M., Nonlinear wave diffraction over submerged obstacles. *Proc. 5th Int. Workshop on Water Waves and Floating Bodies*, Manchester, UK, 1990.
11. Peregrine, D. H. (1972) Flow due to vertical plate moving in a channel, Unpublished note, Department of Mathematics, University of Bristol.
12. Roberts, A. J., Transient free-surface flows generated by a moving vertical plate. *Q. J. Mech and Appl. Math.*, **40** (1987) 129–158.
13. Longuet-Higgins, M. S. & Cokelet, E. D., The deformation of steep surface waves on water, I: a numerical method of computation. *Proc. Roy. Soc. Lond.*, A**350** (1976) 1–25.

APPENDIX A: SECOND ORDER ANALYTICAL SOLUTION FOR A RECTANGULAR CONTAINER

We consider the two-dimensional transient wave problem in a container of width b and depth d. The origin of the Cartesian system is located on the free surface and at the left hand side of the container. The governing equation and boundary conditions based on the linearized potential theory can be written as

$$\nabla^2\phi = 0 \qquad 0 \le x \le b \qquad -d \le y \le 0 \tag{A1}$$

$$\frac{\partial^2\phi}{\partial t^2} + g\frac{\partial\phi}{\partial y} = 0 \qquad y = 0 \tag{A2}$$

$$\frac{\partial\phi}{\partial y} = 0 \qquad y = -d \tag{A3}$$

$$\frac{\partial\phi}{\partial x} = 0 \qquad x = 0 \quad \text{or} \quad x = b \tag{A4}$$

The initial condition is given as

$$\begin{aligned} &\phi(x, y = 0, t = 0) = \psi(x) \\ &\eta(x, t = 0) = -\frac{1}{g}\frac{\partial\phi(x, y = 0, t = 0)}{\partial t} = \xi(x) \end{aligned} \tag{A5}$$

It is evident that the solution of the above equation can be written as

$$\phi = \sum_{m=0}^{\infty} F_m(t)\frac{\cosh k_m(y + d)}{\cosh k_m d}\cos k_m x \tag{A6}$$

where $k_m = m\pi/b$. Using eqn (A2) we obtain

$$F_m(t) = A_m \cos\omega_m t + B_m \sin\omega_m t \tag{A7}$$

where

$$\omega_m = [k_m g \tanh(k_m d)]^{1/2} \tag{A8}$$

Substituting eqns (A6) and (A7) into (A5), we have

$$\begin{aligned} A_m &= \frac{2}{b}\int_0^b \psi(x)\cos k_m x\,\mathrm{d}x \\ B_m &= -\frac{2g}{b\omega_m}\int_0^b \xi(x)\cos k_m x\,\mathrm{d}x \end{aligned} \tag{A9}$$

For the case of

$$\psi(x) = 0 \qquad \xi(x) = a\cos(2\pi x/b) \tag{A10}$$

eqn (A9) becomes

$$A_m = 0 \qquad B_2 = -ag/\omega_2 \qquad B_m = 0 \quad (m \ne 2) \tag{A11}$$

This leads to

$$\eta(x, t) = a\cos\omega_2 t\cos k_2 x \tag{A12}$$

To investigate the nonlinear problem we can use a Stokes perturbation expansion of the velocity potential, and for this particular case we may obtain an analytical expression for the second order potential ϕ_2 as follows. The second order potential satisfies eqns (A1), (A3) and (A4) and the following free surface boundary condition

$$\begin{aligned} \frac{\partial^2\phi_2}{\partial t^2} + g\frac{\partial\phi_2}{\partial y} = &-\eta_1\frac{\partial}{\partial y}\left[\frac{\partial^2\phi_1}{\partial t^2} + g\frac{\partial\phi_1}{\partial y}\right] \\ &-\frac{\partial}{\partial t}(\nabla\phi_1)^2 \qquad y = 0 \end{aligned} \tag{A13}$$

where ϕ_1 and η_1 on the right hand side of the equation are the first order solutions which are obtained from eqns (A6) and (A12). The initial condition for the second order potential can be given as

$$\phi_2(x, y = 0, t = 0) = 0 \qquad \eta_2(x, t = 0) = 0 \tag{A14}$$

where

$$\eta_2 = -\frac{1}{g}\left(\frac{\partial\phi_2}{\partial t} + \eta_1\frac{\partial^2\phi_1}{\partial y\partial t} + \frac{1}{2}\nabla\phi_1\nabla\phi_1\right) \tag{A15}$$

Using the solutions for ϕ_1 and η_1, we obtain

$$\frac{\partial^2\phi_2}{\partial t^2} + g\frac{\partial\phi_2}{\partial y} = -\frac{1}{4}\frac{a^2}{\omega_2}\sin 2\omega_2 t[3\omega_2^4 + k_2^2 g^2 + 3(\omega_2^4 - k_2^2 g^2)\cos 2k_2 x] \quad y = 0 \quad \text{(A16)}$$

Thus

$$\phi_2 = \frac{1}{16}\frac{a^2}{\omega_2^3}(3\omega_2^4 + k_2^2 g^2)\sin 2\omega_2 t + \frac{1}{16}\frac{a^2}{\omega_2^3}(\omega_2^4 - k_2^2 g)^2 \times \frac{\cosh 2k_2(y+d)}{\cosh 2k_2 d}\cos 2k_2 x \sin 2\omega_2 t + D_0 t + \sum_{m=1}^{\infty} D_m \sin\omega_m t \frac{\cosh k_m(z+d)}{\cosh k_m d}\cos k_m x \quad \text{(A17)}$$

The initial condition leads to

$$D_0 = -\frac{1}{8}\frac{a^2}{\omega_2^2}(k_2^2 g^2 - \omega_2^4)$$
$$D_4 = \frac{1}{8\omega_4}\frac{a^2}{\omega_2^2}(k_2^2 g^2 + 3\omega_2^4) \quad \text{(A18)}$$

with all other coefficients being zero.

The second order wave elevation can be obtained from eqn (A15). At the centre of the container, it becomes

$$\eta_2 = \frac{1}{8g}\left(2(\omega_2 a)^2\cos 2\omega_2 t + \frac{a^2}{\omega_2^2}(k_2^2 g^2 + \omega_2^4) - \frac{a^2}{\omega_2^2}(k_2^2 g^2 + 3\omega_2^4)\cos\omega_4 t\right) \quad \text{(A19)}$$